OBSERVATION OF PIPELINE BEHAVIOR AT GEOGRAPHICALLY COMPLEX SITE DURING EARTHQUAKES

K. Tsukamoto (I)
N. Nishio (II)
M. Satake (III)
T. Asano (IV)
Presenting Author: K. Tsukamoto

SUMMARY

Observation of the behavior of a pipeline during earthquakes has been carried out at a site where the subsurface ground structure along the pipeline is remarkably changing. Observed strains in the pipeline are always the greatest at the boundaries between original rigid soils and less rigid soils with which a valley had been filled to reclaim the land. The analysis of data shows that the most essential cause of strain is a non-uniform response of ground to S wave due to non-uniformity of the ground. While, surface waves are shown to be a minor cause.

INTRODUCTION

Through the investigations of the damage to buried pipelines during earthquakes, it became evident that damage ratio is the highest in the areas where non-uniformity of surface ground structure is remarkable.[1), 2), 3)] The non-uniformity of ground structure is represented mainly by an abrupt change of the depth of a soft surface layer. In order to investigate the cause of concentration of damage in the areas with non-uniform ground structure, earthquake observation is being carried out using a gas pipeline buried in a reclaimed land at Nankodai near Sendai City where pipelines for both gas and water sustained a great number of damage during Miyagiken-oki earthquake (1978).

OBSERVATION OF DYNAMIC RESPONSE OF PIPELINE

Outline of Ground and Pipeline for Observation

Nankodai area is a residential land reclaimed by means of cutting off the tops of hills and filling the valleys with cut soils. The pipeline for the observation crosses a former valley which had been filled and flattened apparently. The cross section of the filled valley along the pipeline is as shown

(I) Assistant Chief Researcher of Pipeline Engineering Division, R & D Institute, Tokyo Gas Co., Ltd., Tokyo, Japan

(II) Chief Researcher of Pipeline Engineering Division, R & D Institute, Tokyo Gas Co., Ltd., Tokyo, Japan

(III) Professor of Civil Engineering, Tohoku University, Sendai, Japan

(IV) Instructor of Civil Engineering, Tohoku University, Sendai, Japan

in Figure 1. Soil profile shows that the original (natural) ground is composed of tuffy sandstone and tuff with N-value of greater than 50. While the filled soil, although it originates in the same soil as the original ground, is more or less sandy containing soft conglomerate up to about 100 mm in size, and its N-values range from 2 to 21.
The velocities of S wave measured by PS loggings are 160 to 350 m/s in the filled soil and 630 m/s in the original ground. Predominant frequencies of the ground by means of micro tremor measurement at the location of the deepest filled soil ranges from 2.0 to 8.0 Hz, and high peaks are observed between 3.0 and 5.0 Hz. While, measurements on the original ground do not show clear peaks of predominant frequency.
The pipe for the observation is a steel pipe of 216.3 mm in outside diameter with wall thickness of 5.8 mm.

Observation System

The locations of accelerometers and strain gages are as shown in Fig. 1. Observations are made by use of an automatic data recording system which is put into operation by a weak signal of earthquake taken by the accelerometer GA 1.

Summary of Observed Records

Maximum accelerations and maximum strains observed during sixteen earthquakes are summarized in Table 1. The value of maximum accelerations of the pipeline is almost the same as that of the ground, and maximum accelerations of both the ground and the pipeline always take place between the section of filled soil (i.e., at GA 2, PA 1 and PA 2). Maximum strains in the pipeline take place at the boundaries between the original ground and the filled soil (i.e., at PS 7 and PS 3) in most cases, and the values of bending strains are always less than 1/5 of those of axial strains except for the case of feeble earthquakes. The distributions of the axial strains along the pipeline are shown in Fig. 2. A remarkable feature that the strain always take the maximum value around the both boundaries between the original ground and the filled ground is observed.

ANALYSIS OF RECORDS

Fig. 3 shows power spectra calculated from the waveform records of accelerations and strains during two earthquakes (No. 14 and 15 in Table 1) which induced the greatest strains in the pipeline throughout the observation. Earthquake No. 14 may be regarded as an example of distant earthquakes which usually contain considerably strong power in low frequency region. The power spectra of the records both GA 1X and GA 3X (both accelerometers, GA 1 and GA 3, are in the original ground. The letter X denote the direction of pipeline axis) in Fig. 3, a) show the predominance of low frequency component (0.88 Hz). In contrast, earthquake No. 15 shows a typical feature of short distance earthquakes. Very high-frequency components are predominant in this earthquake as shown in the power spectra for both GA 1X and GA 3X in Fig. 3, b). Comparison between the power spectra for GA 2X and GA 1X shows the amplification of earthquake motion by the stratum of the filled soil. The components with frequencies around 4.0 Hz are greatly amplified during the both earthquakes. This frequency agrees with the predominant frequency of the filled

soil stratum inferred from micro tremor characteristics. In contrast, frequency components both higher than and lower than 4.0 Hz are considerably suppressed. The power spectra for PA 2X for the both earthquakes show frequency distribution intermediate between the power spectrum for GA 2X and that for GA 3X. Power spectra for strain waveforms in the pipeline show a remarkable feature; predominant frequencies in the strain waveform at PS 7 (and PS 3 as well), which showed the maximum strains during the both earthquakes, are in almost perfect agreement with those in the acceleration waveform at GA 2. On the other hand, power spectra of the strains at PS 5 and PS 9 do not show such remarkable feature as in the case of PS 7 (and PS 3), and the power is less intense than that of the strains at PS 7 (and PS 3).

The above facts show that the strain in the pipeline is mainly caused by the difference in the motions between the filled soil and original ground, and the magnitude of the strain is mainly determined by the intensity of the motion of the filled soil.

Fig. 4 shows a result of disintegration of strain waveforms for the same earthquakes. The original waveforms of acceleration and strain at representative locations are disintegrated into three frequency ranges of components. As for Earthquake No. 14, the low frequency band (0 to 2.0 Hz) component of the acceleration at the original ground (GA 3X) shows almost the same intensity as the medium frequency band (2.0 to 5.0 Hz) component. However, it remains almost constant in intensity throughout all locations (GA 3X, GA 2X, and PA 2X), while the medium frequency component is greatly amplified by the filled soil (GA 2X). Waveform of each frequency band component of the strain (PS 7) closely resembles to the corresponding component of the acceleration of the filled soil. High frequency band (5.0 to 10.0 Hz) component is quite feeble.
In contrast, Earthquake No. 15 shows intense high frequency band (5.0 to 25.0 Hz) component in the acceleration waveform at the original ground, while low frequency component is very little. The amplification of medium frequency component by the filled soil is just as in the case of Earthquake No. 14. It is shown that the contribution of the high frequency component to the strain in the pipeline is relatively less.

The both earthquakes, although their frequency characteristics are different from each other, show a common feature that the medium frequency band component of the vibration which correspond to the natural frequencies (i.e. predominant frequencies by micro tremor measurement) of the filled soil contribute to the major part of the magnitude of strain in the pipeline. From Fig. 4, it is known that more than 60% of the value of the maximum strain is due to the medium frequency component in the both earthquakes.

CONCLUSIONS

Earthquake observation on a pipeline which crosses a valley filled with relatively less rigid soil showed a peculiar pattern of distribution of strain in the pipeline as shown in Fig. 2. Both power spectra analyses and frequency band analyses could explain the cause of the peculiarity of strain distribution. The causes and the characteristics of strain in a pipeline during an earthquake are summerized as follows:

(1) The greater part of the strain is mainly due to the existence of grounds with different vibration characteristics.

(2) The maximum strain in the pipeline takes place around the boundary between a soft ground and a rigid ground.

(3) The greater part of the magnitude of the strain is mainly determined by the response of the soft soil stratum to an earthquake; this implies that the response of the ground to the S wave is the most important factor for the prediction of strains in pipelines, and the surface wave is less important.

REFERENCES

1) Okamoto, S., "Introduction to Earthquake Engineering", University of Tokyo Press.

2) Kubo, K., Katayama, T., and Sato, N., "Quantitative analysis of Seismic Damage to Buried Pipelines", Proceedings of the 4th Japan Earthquake Engineering Symposium, Nov. 1975.

3) Nishio, N., "Analysis of Pipeline Damage by Earthquakes Using Probabilistic Ground Displacement Model", Proceedings of the 4th International Conference on Pressure Vessel Technology, May 1980.

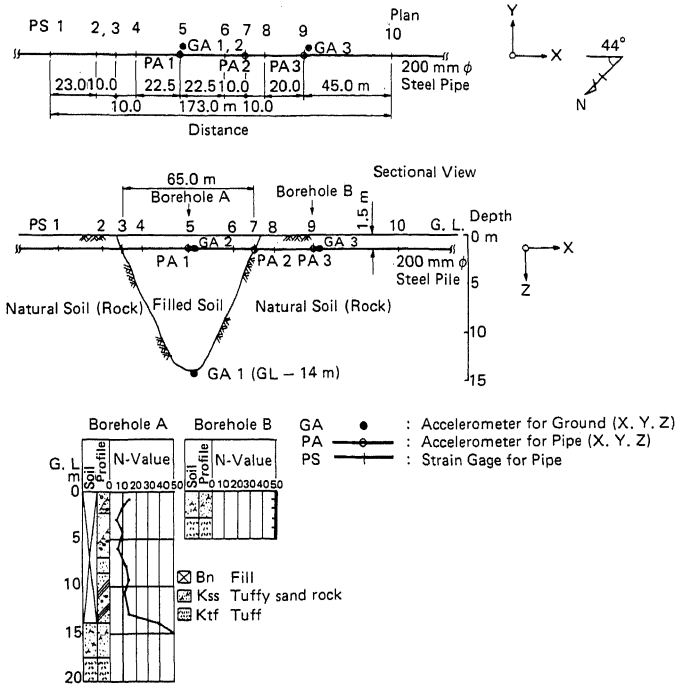

Fig. 1 Soil Profile and Location of Measuring Instruments

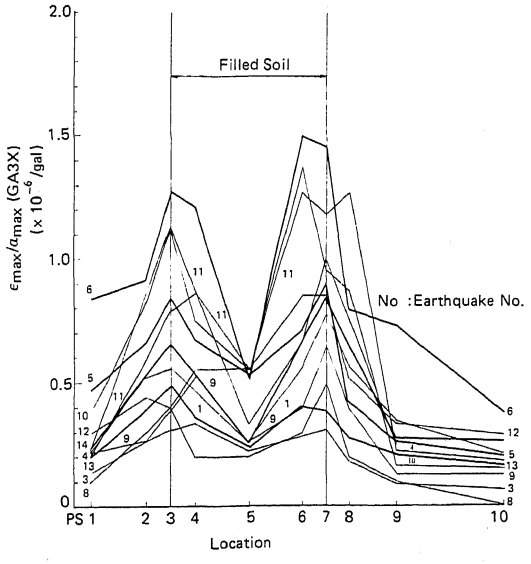

Fig. 2 Distribution of Axial Strain along Pipeline (Strain is normalized with respect to unit ground acceleration (GA 3))

Table 1 Summary of Records of Observed Earthquakes

EQ KE No.	Date and Time	Location of Focus N	Location of Focus E	Depth of Focus (km)	Epicentral Distance (km)	Magnitude (M)	JMA Intensity Sendai (Nankodai)	Max. Acceleration (gal)* X	Max. Acceleration (gal)* Y	Max. Acceleration (gal)* Z	Max. Pipe Strain** (x 10^{-6}) Axial	Max. Pipe Strain** (x 10^{-6}) Bending
1	1981 9.26 00:02	Off Miyagi Pref. 38.4°	143.2°	40	200	6.1	I	3.3 (2)	5.0 (2)	1.2 (2)	1.8	0.3
							(II)	2.7 (1)	3.9 (1)	1.0 (2)	(7)	(5)
2	9.28 12:38	Far Off Sanriku 40.2	143.5	40	290	–	0	0.7 (2)	1.0 (2)	0.2 (2)	0.5	0
							(I)	0.6 (1)	0.8 (2)	0.0 (–)	(7)	(–)
3	10.12 01:35	Off Miyagi Pref. 38.6	142.1	40	100	4.5	I	5.4 (2)	6.8 (2)	3.7 (2)	1.5	0.3
							(II)	7.2 (2)	8.1 (2)	6.7 (2)	(4)	(7)
4	10.15 10:48	Off Iwate Pref. 40.3	142.3	40	250	6.0	II	3.8 (2)	3.0 (2)	1.6 (2)	1.5	0.3
							(III)	3.0 (1)	2.8 (1)	1.4 (1)	(7)	(3)
5	11.6 13:34	Off Miyagi Pref. 38.0	141.5	40	65	5.1	II	12.8 (2)	13.5 (2)	8.3 (2)	8.6	1.0
							(III)	12.7 (2)	16.5 (2)	12.0 (2)	(7)	(3, 7)
6	12.2 15:25	Easten off Aomori Pref. 40.8	142.3	40	300	6.6	I	7.5 (2)	9.0 (2)	5.2 (2)	7.2	1.0
							(III)	7.3 (1)	9.9 (1)	5.9 (1)	(6)	(6)
7	12.12 05:02	Far off Sanriku 38.8	143.4	20	220	5.9	0	1.0 (2)	1.2 (2)	0.3 (2)	0.3	0
							(I)	0.9 (1)	1.2 (1)	0.2 (1)	(7)	(–)
8	1982 1.8 05:38	Middle Akita Pref. 40.0°	140.5°	0	185	4.9	0	1.3 (2)	1.5 (2)	1.0 (2)	0.5	0.1
							(I)	1.2 (2)	1.6 (1)	0.9 (1,2)	(7)	(7)
9	1982 1.8 17:03	Off Fukushima Pref. 37.8	142.0	40	110	4.9	0	3.2 (2)	4.3 (2)	3.6 (2)	1.5	0.2
							(II)	3.1 (1,2)	5.0 (2)	4.7 (2)	(7)	(7)
10	3.4 22:13	Off Fukushima Pref. 37.2	142.0	30	165	5.0	0	3.6 (2)	3.9 (2)	3.3 (2)	3.3	0.8
							(II)	3.6 (2)	4.1 (1)	3.8 (2)	(6)	(7)
11	3.7 08:14	Kashima-nada 36.5	140.7	60	210	5.5	0	3.2 (2)	4.0 (2)	3.1 (2)	2.8	0.9
							(II)	3.4 (1)	5.1 (2)	4.3 (2)	(6, 8)	(7)
12	3.21 11:32	Off Urakawa 42.1	142.6	40	450	7.1	0	4.1 (2)	4.5 (2)	2.5 (2)	2.3	0.8
							(II)	3.8 (1)	4.3 (1)	2.0 (1)	(6, 7)	(7)
13	6.1 05:13	Off Miyagi Pref. 38.7	142.2	40	115	6.3	II	22.0 (2)	34.8 (2)	20.0 (2)	9.0	1.2
							(IV)	21.7 (1)	44.3 (2)	22.9 (2)	(3)	(2)
14	7.23 23:23	Off Ibaraki Pref. 36.3	141.7	40	240	7.0	III	30.0 (2)	29.8 (2)	10.5 (2)	15.0	2.3
							(IV)	29.6 (1)	32.1 (1)	9.4 (1)	(7)	(3)
15	8.23 14:50	Off Fukushima Pref. 37.7	141.6	60	90	5.3	III	31.0 (2)	25.6 (2)	15.2 (2)	11.0	1.0
							(IV)	25.0 (2)	18.6 (1)	17.7 (2)	(7)	(3, 7)
16	1983 5.26 12:00	Middle Japan Sea 40.4	139.1	14	295	7.7	III	16.3 (2)	18.7 (2)	8.0 (2)	9.0	1.4
							(III)	13.5 (1)	16.5 (1)	7.5 (1)	(7)	(7)

Notes: *1. Upper case: Max. Acc. of Ground
Lower case: Max. Acc. of Pipe
2. Figures in Parentheses shows the Locations of Accelerometers.
**1. Figures in Parentheses shows the Location of Strain Gage.

a) Earthquake No. 14 (Distant Earthquake)

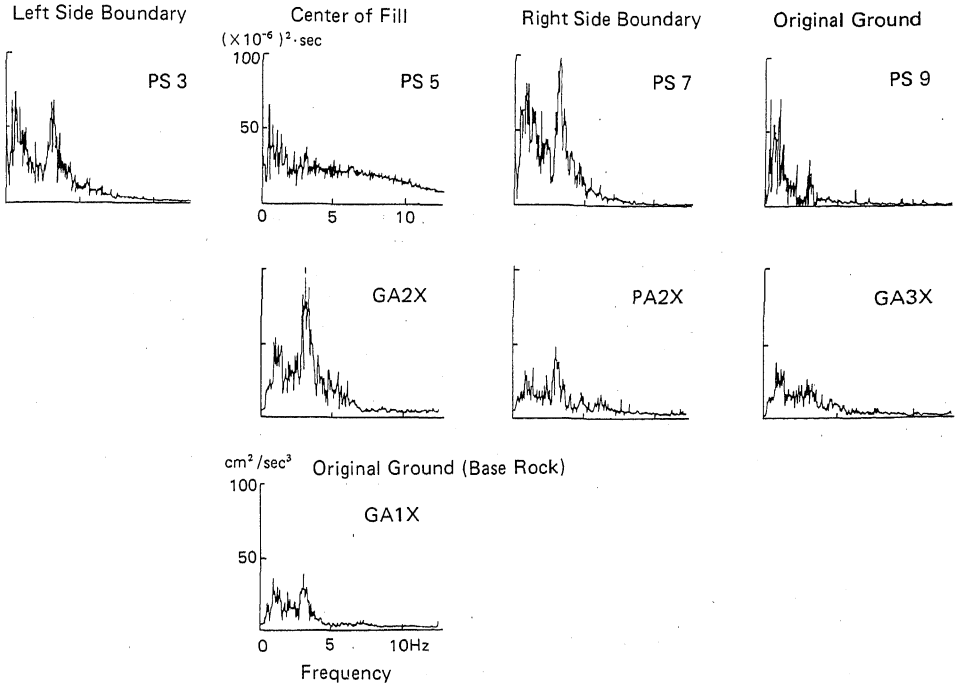

b) Earthquake No. 15 (Short Distance Earthquake)

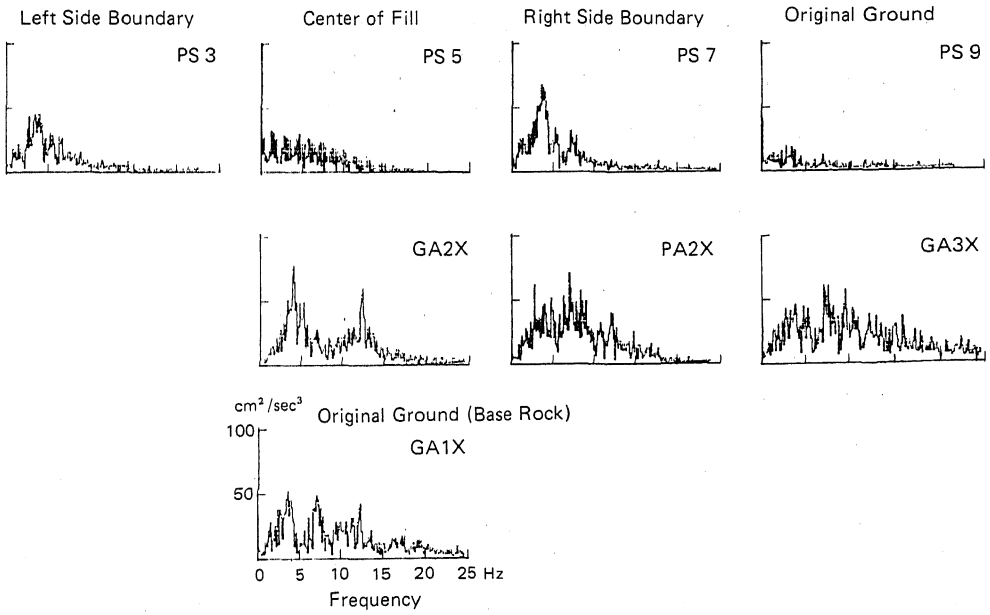

Fig. 3 Power Spectra of Accelerations and Strains during Two Representative Earthquakes

a) Earthquake No. 14 (Distant Earthquake)

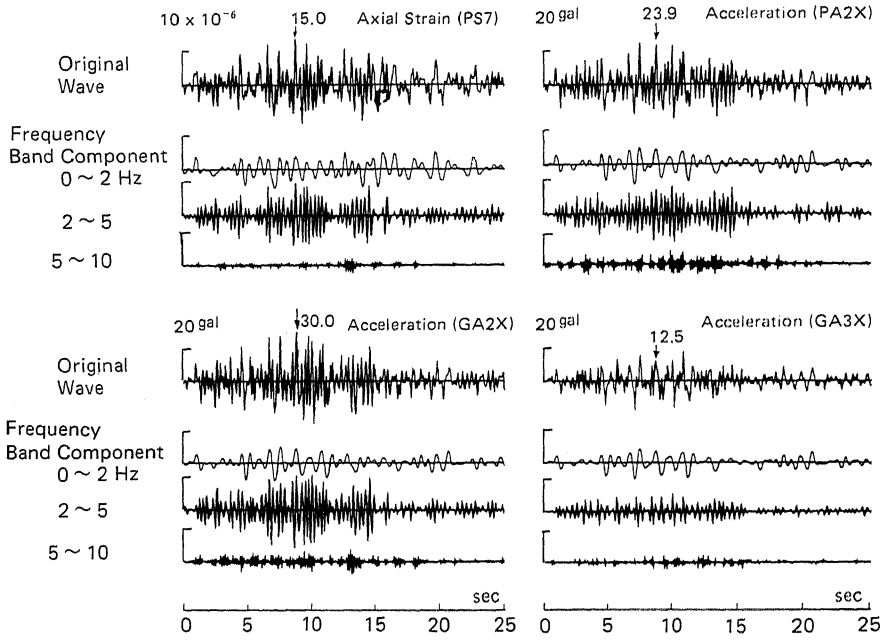

b) Earthquake No. 15 (Short Distance Earthquake)

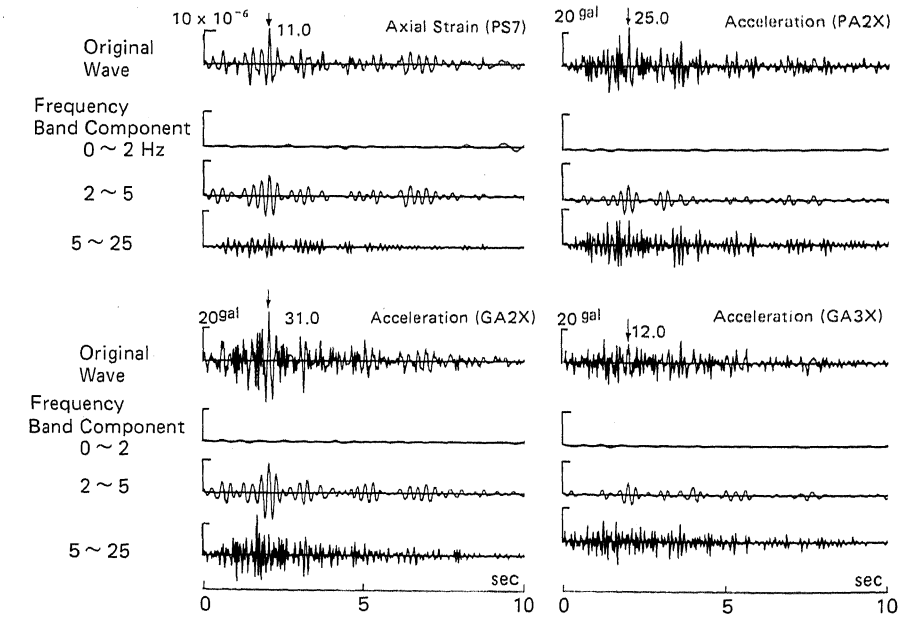

Fig. 4 Disintegration of Strain Waveform into Frequency Band Components